

Discontinuous transitions of social distancing.

R. Arazi and A. Feigel*

Racah Institute of Physics, The Hebrew University, 9190401 Jerusalem, Israel

The 1st wave of COVID-19 changed social distancing around the globe: severe lockdowns to stop pandemics at the cost of state economies preceded a series of lockdown lifts. To understand social distancing dynamics it is important to combine basic epidemiology models for viral unfold (like SIR) with game theory tools, such as a utility function that quantifies individual or government forecast for epidemic damage and economy cost as the functions of social distancing. Here we present a model that predicts a series of discontinuous transitions in social distancing after pandemics climax. Each transition resembles a phase transition and, so, maybe a general phenomenon. Data analysis of the first wave in Austria, Israel, and Germany corroborates the soundness of the model. Besides, this work presents analytical tools to analyze pandemic waves.

I. INTRODUCTION

Pandemics are complex medical and socioeconomic phenomena[1, 2]: near social interactions benefit both spread of disease and significant part of modern economy[3, 4]. During COVID-19 most government and individuals accepted significant limitation on interpersonal contacts (aka social distancing) to reduce pandemics at the cost of the economy. Can the dynamics of social distancing be explained as a self-contained socio-epidemiological model[5–7] or completely subjected to extrinsic effects[8] is a crucial question for sociophysics, a field that tries to describe social human behavior as a physical system.

Social distancing changes as pandemic unfolds, reflecting a change in personal and government beliefs in the future. The spread of disease increases the individual probability to become sick and may collapse the national health system. Social distancing reduces interpersonal interactions and complicates some individual production. The level of social distancing corresponds to equilibrium between future beliefs on epidemic size and economy cost[9, 10].

To address social distancing classical epidemiological modeling is extended with economy or game theory tools[5–7, 11, 12]. SIR model[13] addresses disease spread as gas or network-like[14] interaction of susceptible, infected, and recovered individuals. An infected transmit the disease to susceptible from the moment of infection until he/she recovers. Social distancing reduces inter-person interaction and thus reduces the effectivity of transmission, but at the same time claims significant economic price. To find an equilibrium level of social distancing a utility function quantifies the negative weight of epidemics, social distancing itself, and the economic cost of social distancing. Utility function extension of the SIR model is in the focus of game theory treatment of vaccine policies[15] and recent estimates of COVID-19 economy damage due to social distancing[4, 9, 10, 16–18].

Here we show that social distancing during a pandemic may have discontinuous changes that to some extent resemble phase-transitions. In this work, epidemic starts to unfold according to the SIR model. At each moment social distancing depends on utility functions that quantify the final epidemic size and social distancing economy cost. Optimal values of social distancing correspond to the maxima of the utility function. Discontinuous transitions correspond to the abrupt changes in maxima locations. This work presents an analytical expression of the general utility function in a polynomial form. Utility function, so, reminds the free energy of a system during Ginzburg-Landau phase transition[19–22] and may have some level of universality.

The first component of the utility function is economic gain or loss from a decrease or increase of social distancing. Thus social distancing parameter should address changes in the number of individuals that produce or take place in productive mingling[9, 23].

This work associates social distancing with $s_{th} = 1/R$, where R is a basic reproductive number. R is a major parameter of the SIR model - the average number of susceptible that an infected person infects. Epidemic breaks out when $R > 1$. Network interpretation maps SIR model on a network with edge occupancy $T = 1 - \exp(-s_{th})$ [14]. A utility function, as all other parameters of the model, depends on network topology and s_{th} . This work considers only changes in s_{th} . Association of social distancing transitions only with s_{th} is supported by the fit of COVID-19 data.

The second component of the utility function comprises epidemic cost that favors social distancing. In this work, this cost corresponds to individual future probability to become sick. This probability is proportional to the forward amount of infected till the end of epidemic wave - Final Epidemic Size (FES). An important contribution of this work is an analytical presentation of FES derivatives due to basic reproductive number with the help of Lambert W function[24–26].

The work proceeds with the presentation of the SIR model with induced transitions (SIRIT), almost analytical treatment of this model, the calibration of an epidemic and economy parameters of the model using time

* sasha@phys.huji.ac.il

series of active cases and causalities during the 1st wave of COVID-19 in Austria, Israel, and Germany, followed by a discussion of obtained results and their implications.

II. SIRIT MODEL

Classical SIR model separates the population in three compartments: S susceptible, I infected and R recovered. The flux between compartments goes in the order $S \rightarrow I \rightarrow R$ since susceptible becomes infected at frequency β^{-1} during an encounter with an infected one. Infected becomes recovered after time γ^{-1} on average. The population is well mixed and sustains the gas-like interaction of its members.

During COVID-19 pandemics, daily worldwide reports[27] include active cases and coronavirus deaths. Active cases are detected infected, which are a fraction of the total infected. Thus in this work, we redefine I as active cases, and instead of recovered R will use deceased $D = MR$, where M is Infected Fatality Rate (IFR). IFR is an average probability of an infected to die (for instance, reported Covid-19 IFR in Germany $M \approx 0.37\%$ [28]).

Here are SIR equations modified to this work:

$$\begin{aligned} \frac{\partial s}{\partial t} &= -\beta A s I, \quad A = \frac{A'}{N}, \\ \frac{\partial I}{\partial t} &= \beta I(s - s_{th}), \quad s_{th} = \frac{\gamma}{\beta} = \frac{1}{R} \\ \frac{\partial D}{\partial t} &= \beta s_{th} N A I M \end{aligned} \quad (1)$$

where I is reported absolute amount of active cases[27], A' is a ratio between actual and reported active cases, N is the population size, $0 < s < 1$ is the normalized ($s = \frac{S}{N}$) amount of susceptible and D are reported deaths due to epidemy. When population size N and A' remain constant it is convenient to unite them into a single parameter $A = \frac{A'}{N}$.

The parameter s_{th} represents social distancing in this work. It also represents a threshold value to ratio of susceptible in population: number of infected growths when $s > s_{th}$ and reduces when $s < s_{th}$. Besides $s_{th} = 1/R$, where $R = \beta/\gamma$ is basic reproduction number.

In this work s_{th} changes with time according to utility function $U(s_{th})$. At each moment t the value of $s_{th}^{current}$ changes if there exists s_{th}^{new} such that:

$$U(s_{th}^{new}) > U(s_{th}^{current}). \quad (2)$$

The utility function consists of two parts that represent pandemics cost C and economy gain G :

$$U = C + G, \quad (3)$$

where C is proportion to epidemy size FES[15, 29]:

$$C = -A\beta \int_t^\infty I dt. \quad (4)$$

Epidemy cost changes with time as population advances in (s, I) space.

Economy gain is some general function $G(s_{th})$. Let us expand economy gain in Taylor series around $s_{th}^{current}$:

$$G(\Delta s_{th}) = G(s_{th}^{current}) - A_{open} \Delta s_{th}^- - A_{close} \Delta s_{th}^+ + B_{open} (\Delta s_{th}^-)^2, \quad (5)$$

where $\Delta s_{th} = s_{th} - s_{th}^{current}$, Δs_{th}^- and Δs_{th}^+ are negative and positive value of Δs_{th} . The parameters $A_{open}, A_{close}, B_{open}$ are some positive economy weights that are independent of epidemy clinics. Utility function is asymmetric in Δs_{th}^- and Δs_{th}^+ because of higher economic price of a lockdown than price of later release. Major assumption of this work is that $A_{open}, A_{close}, B_{open}$ remain constant at least from epidemy climax (greatest number of infected) until the first major change of social distancing.

Epidemy cost C is expanded in Taylor series of the third order:

$$C = C(s_{th}^{current}) - a \Delta s_{th} - b \Delta s_{th}^2 - c \Delta s_{th}^3. \quad (6)$$

Coefficients a, b, c (as epidemy cost itself (4)) depend on s_{th}, s, I . Expansion of the third order, unlike the second order in (5), required due to non-linear behavior of FES (4) and because pandemic cost prevents significant lift of social distancing constraints (the third term in (6)).

This work considers only a decrease in social distancing $\Delta s_{th} < 0$ which corresponds to the reopening of the economy. It is a consequence of an assumption that $A_{close} \gg A_{open}$ - even small constraint on social interactions bring significant economy damage. Transition occur if utility function (4), taking into account (5) and (6):

$$U = -(a + A_{open}) \Delta s_{th} - (b - B_{open}) \Delta s_{th}^2 - c \Delta s_{th}^3, \quad (7)$$

possesses any positive values for $\Delta s_{th} < 0$. To consider only relative changes in s_{th} , we set $U(s_{th}^{current}) = 0$.

Utility function (7) together with condition (2) possesses Ginzburg-Landau like instability, see Figure 1. First, no transition occurs if $U < 0$ for all s_{th} . Second, discontinuous change in s_{th} take place if there is single value $U(s_{th}) > 0$. Third, s_{th} changes continuously when derivatives of (7) vanish near $\Delta s_{th} = 0$ ($a + A_{open} = b - B_{open} = 0$).

Discontinuous transition occurs when there exists a single $\Delta s_{th} < 0$ root for $U = 0$ (7). This condition requires the determinant of quadratic function $U/\Delta s_{th}$ (7) to vanish:

$$4c(a + A_{open}) = (b - B_{open})^2. \quad (8)$$

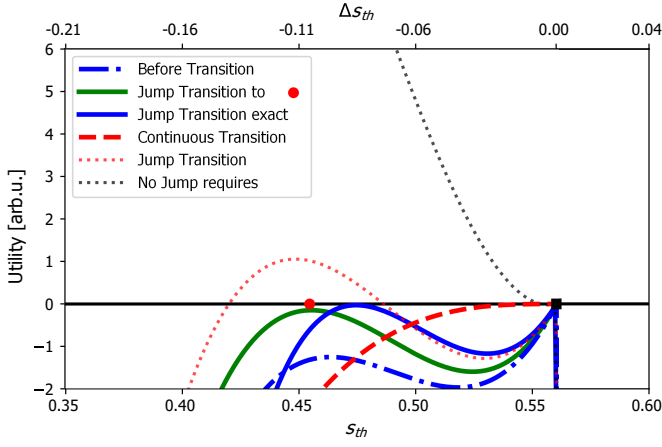


Figure 1. Utility as a function of social distancing before, during and after transition takes place. A measure of social distancing is $0 < s_{th} < 1$. Transition occur between current value of $s_{th}^{current}$ (black square) to its new value s_{th}^{new} (red circle) when $U(s_{th}^{new}) > U(s_{th}^{current})$ ($U(s_{th}^{current}) = 0$). Before transition $U(s_{th}^{current})$ is the highest value of the utility function. Then there are two possibilities: Discontinuous change $s_{th}^{new} \neq s_{th}^{current}$ (solid green line) or continuous change $s_{th}^{new} \approx s_{th}^{current}$ (dashed red line). Two cases (dotted lines) that make possible change of s_{th} to many values do not exist because either continuous or discontinuous transition occur before. This work considers only opening of population, that corresponds to reduction of s_{th} . Utility function is approximately a cubic function of Δs_{th} (solid green). The transition predicted by exact calculation (solid blue) predict insignificant for this work changes in time and strength of the transition.

The corresponding Δs_{th} :

$$\Delta s_{th} = \frac{b - B_{open}}{2c}. \quad (9)$$

The new s_{th}^{new} is:

$$s_{th}^{new} = s_{th}^{current} + \Delta s_{th}. \quad (10)$$

Coefficients a, b, c possess an analytic approximation, while condition (8) reduces to a polynome of the 4th order.

III. MAIN ANALYTICAL PROPERTIES

The first two equations of (1) have a solution in the form of Lambert W function[24–26]:

$$s = -s_{th}W\left(-\frac{s_0}{s_{th}}\exp\left[\frac{A(I - I_0) - s_0}{s_{th}}\right]\right), \quad (11)$$

where (s_0, I_0) are initial values for ratio of susceptible s and amount of infected I correspondingly, see Appendix A. Eq. (11) is valid for any (s, I) on the trajectory in time that initiates at (s_0, I_0) . The parameter s reaches

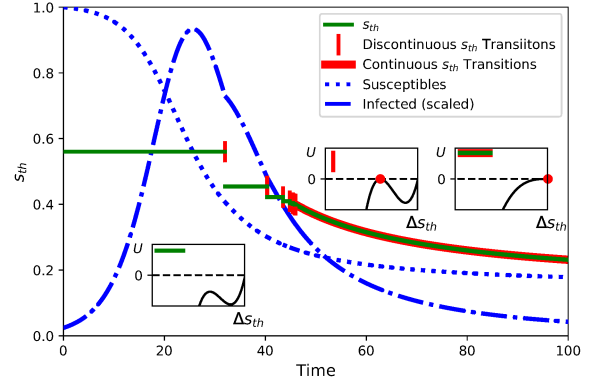


Figure 2. Epidemy wave dynamics with social distancing transitions. SIR predicts wave-like behavior of infected individuals (dash-dotted blue) accompanied by reduction of susceptible ones (dotted blue). An utility function caused changes in social distancing parameter s_{th} (solid green). Transition (red bars) occur when there exists new value of s_{th}^{new} such that utility function $U(s_{th}^{new}) > 0$. Form of utility function before and during transition are show in subplots. Region of continuous transitions follows the series of discontinuous ones. Changes in s_{th} cause time derivative discontinuities in dynamics of infected and susceptibles.

its smallest value s_{min} when there are no more infected ($I = 0$) at $t = \infty$:

$$s_{min} = -s_{th}W\left(-\frac{s_0}{s_{th}}\exp\left[-\frac{AI_0 + s_0}{s_{th}}\right]\right). \quad (12)$$

Following (1), FES at any time t is:

$$A\beta \int_t^\infty I dt = -\log s|_{s(t)}^{s_{min}}, \quad (13)$$

and parameters a, b, c in (6) are the Taylor coefficients:

$$a = -\frac{\partial \log s_{min}}{\partial s_{th}}, b = -\frac{1}{2} \frac{\partial^2 \log s_{min}}{\partial s_{th}^2}, c = -\frac{1}{6} \frac{\partial^3 \log s_{min}}{\partial s_{th}^3}. \quad (14)$$

The parameters (14) are polynomials of $\log s$ of the order 1, 2 and 3 correspondingly, see Appendix B. Thus condition (8) is a polynomial of the 4th order (quartic function) of $\log s$, with coefficients that are the functions of $(s_0, I_0, s, I, s_{th}, \beta, A)$.

Consider population at state $(s_0, I_0, s, I, s_{th}, \beta, A)$. To calculate time to transition as a function of A_{open}, B_{open} one need to solve 4th order equation (8) to find s_{tr} of transition (closest to 0 real root of (8)), calculate Δs_{th} of transition using (9) then calculate the time to transition:

$$\int_s^{s_{tr}} \frac{ds}{\frac{ds}{dt}} = \int_s^{s_{tr}} \frac{ds}{-\beta A \left[I_0 + \frac{1}{A} \left[s_0 - s + s_{th} \log \left[\frac{s}{s_0} \right] \right] \right]} s \quad (15)$$

between current value s and s_{tr} .

A function T :

$$s_{tr}, s_{th}^{new} = T(s_0, I_0, s, I, s_{th}, \beta, A, A_{open}, B_{open}), \quad (16)$$

summaries results of the previous paragraph. T returns future value of $s=s_{tr}$ where transition of $s_{th} \rightarrow s_{th}^{new}$ will take place. The follow up transition follow T , after update of $(s_0, I_0, s, I, s_{th}) \rightarrow (s_{tr}, I(s_{tr}), s_{tr}, I(s_{tr}), s_{th}^{new})$.

Many transitions (16) result in Zeno phenomenon - the system making an infinite number of transition in a finite amount of time, see Figure 2. Transitions of s_{th} take place until (16) predicts $\Delta s_{th} = 0$. Following (8) and (9) it happens when the first two derivatives of (7) vanish: $(a - A_{open} = b - B_{open} = 0)$. The time to these infinite number of transitions to take place remain finite because time is finite to pass between and two values of s , see (15).

After the limit of transition, utility function preserves continuous transition state. Otherwise if s_{th} remain constant the utility function would make possible many values of s_{th} with $U(s_{th}) > 0$, see Figure 1. At the region of continuous transitions, at each moment equation:

$$a = -A_{open} \quad (17)$$

defines s_{th} , and (1) is solved numerically.

Transitions of s_{th} result in time derivative discontinuities of s and I . These derivative discontinuities can be detected, see Figure 2.

IV. FIT

SIRIT model provided a successful fit of COVID-19 data in Austria, Germany and Israel. Austria and Israel are countries with similar population sizes and with similar policies during the initial stages of the 1st wave. Germany is a country with about $\times 10$ population size that still demonstrates SIR like behavior during the first wave.

The main purpose of the fit is to show that self-contained model SIRIT is capable of description dynamics of the 1st COVID-19 wave. Full optimization of the

COVID-19 data fit and its validation is out of the scope of this work.

The fit proceeds in the following steps: First, a small region around the greatest number of infected, see Figure 3, calibrates s_0, I_0, β, A . In this work $\gamma = 0.26$, this choice can be quite arbitrary in the boundaries of reported COVID-19 $1/7 < \gamma [day^{-1}] < 1$ values[30].

Second, one can see discontinuous changes in time derivatives of reported active cases, especially as deviations from initial SIR model fit, see the outermost left red bar in Figure 3. This work associates these changes with transitions of social distancing. The time t and s_{tr} of the first transition are detected. New values of β, s_{th} were fitted for an active case during about 20 days after the transition. In all case, fit predicted β to remained unchanged while s_{th} to accept a new value s_{th}^{new} . Third, eq. (16) is solved for A_{open} and B_{open} (e.g. using Nelder-Mead method), when s_{tr} and s_{th}^{new} are the values from the previous step. Fourth, next transitions s_{th}^i , where i is the index of the transition, are calculated using (16) and (17).

Complete dynamics of the first wave active cases and susceptible, see Figure 3, follows eqs. (1) and the fitted $s_0, I_0, s_{th}, \beta, A, N$ together with the transitions locations t_i, s_{tr}^i and strengths s_{th}^i . See Figure 3 for changes in s_{th} .

To fit casualties, an effective population size N is chosen to fit reported coronavirus death at the 100th day of the first wave. It predicted quite small N less than 1/10 Austrian population. This result to be addressed during the discussion. Besides, there exists some time shift between calculated and reported coronavirus death.

Two alternative fits of Austria COVID-19 data are brought in Figure 4. The first demonstrates the sensitivity of the fit to the choice of the first transition. The second demonstrates that for any first transition the entire curve can be fitted if A_{open}, B_{open} are fitted separately for any transition.

The results for Germany and Israel summarized in Figures 5 and 6 together with Table I. Table I summarizes the results for all three countries. All countries demonstrated a low size of the effective population. One of the assumptions that $s_0 \approx 1$. In the case of Israel, it required to be constrained. Neither of deviations from the fit refutes the main results of this work.

V. DISCUSSION

The work introduces SIRIT, a standard Susceptible-Infected-Recovered (SIR) model extended with a utility function that predicts induced transitions (IT) of social distancing. The model provides almost analytical treatment and reasonable but an ambiguous fit of COVID-19 1st wave active cases and casualties. Let's summarize and discuss the main assumptions, results, and implications of this work together with some alternative approaches.

The validity of the predicted discontinuous dynamics of social distancing and results depend on the specific

choice of the social distancing parameter and the choice of a utility function.

The choice of $s_{th} = 1/R$ as a social distancing parameter is not unique. In the framework of SIR, for instance, another valid candidate is β - the probability of disease transmission per unit time[6, 7]. This parameter depends both on clinics of infection and the mechanism of interpersonal interactions. The fit of the first social distancing transitions (deviations from SIR model) after COVID-19 climax in Austria, Germany, and Israel, but, demonstrates that β remains constant during the transitions.

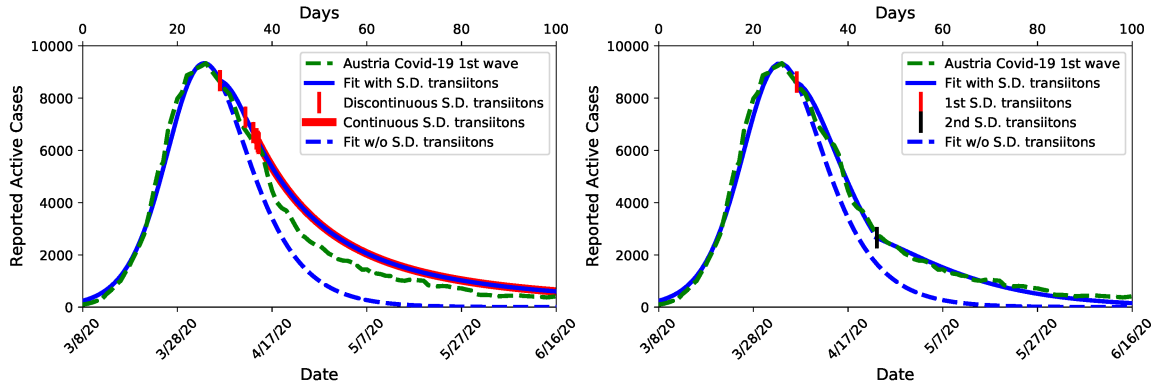


Figure 4. Alternative fits of Austria COVID-19 1st wave A) Fit with different date of the first transition. There is a significant deviation between reported and calculated active cases. It demonstrates that the fit techniques are sensitive to the choice of the first transition. This sensitivity provides a hope that the fit may reveal something real parameters of the population or economy of the state. B) Fit with two different distance transitions. By adjusting utility function weights A_{open}, B_{open} separately for every transition a better fit can be achieved. In the case of Austria, only two transitions are required. This method is less sensitive to the choice of the first transition.

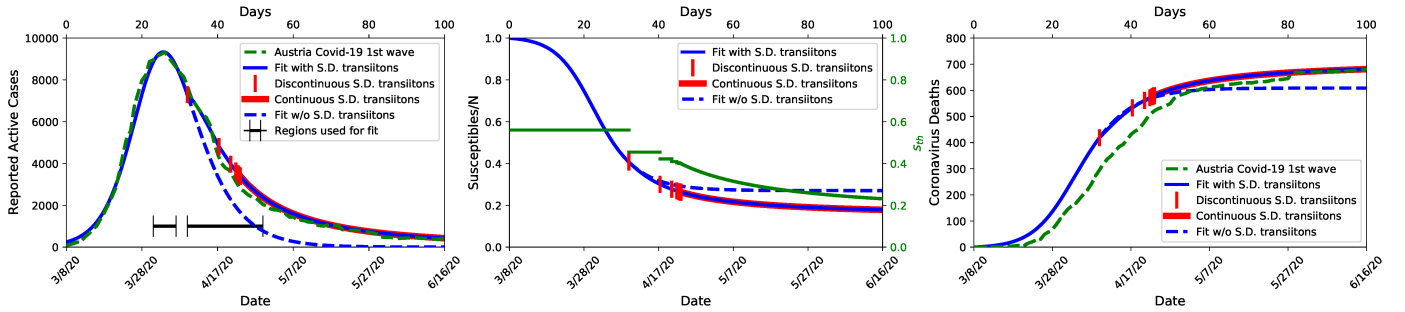


Figure 3. Fit of Austria COVID-19 1st wave with multiple social distancing transitions. The purpose of the fit is to show that there is a possibility to fit the real data using many transitions. A) Active cases - reported (dashed green) and calculated with many transitions (solid blue). Before transitions (red bars) classical SIR fits well the reported active cases. There is a significant deviation of SIR from reported cases after the first transition (dashed blue). SIRIT model with many transitions fit well entire range of the first wave, though the fit was obtained using a small range around the greatest of active cases and characteristics of the first transition (horizontal error bars). B) Susceptibles and Social distance parameter s_{th} . At each transition s_{th} changes its value. Series of discontinuous transitions is followed by a continuous change region. C) Coronavirus deaths. There exists a time delay between reported and calculated deaths. This delay can be explained by the long course of COVID-19.

An interesting conclusion of this work is that change in social distancing corresponds to γ - a rate of becoming immune. Transition corresponds to changes in $s_{th} = \gamma/\beta$ while β remains constant. It seems a fallacy because γ seems to depend only on epidemic clinics. Even so, social distancing affects γ - society on alert removes contagious individuals by distancing from confirmed sick or even from asymptomatic cases that had contact with a sick person.

In an alternative way, $1/s_{th} = R$ can serve as a social distancing parameter. This choice does not change major

predictions or analytical developments of this work. The parameter $0 < s_{th} < 1$ that can be compared with the fraction of susceptible in a population serves better the purpose of this work.

The price of pandemics can go beyond the final epidemic size (FES). For instance, one may include derivatives of infected in time as a psychological factor that affects individual decision making. There is a lot of room to make utility function more complicated. Relative weights of different pandemic characteristics on individual or government decision making is an important question for future investigations and out of the scope of this work.

The first wave of COVID-19 in Austria, Germany, and Israel was fitted using SIRIT in two different ways: The first, series of discontinuous transitions with con-

stant economy parameters. The parameters A_{open}, B_{open} are fitted by the first transition. The second, economic weights are fitted for every candidate transition (devia-

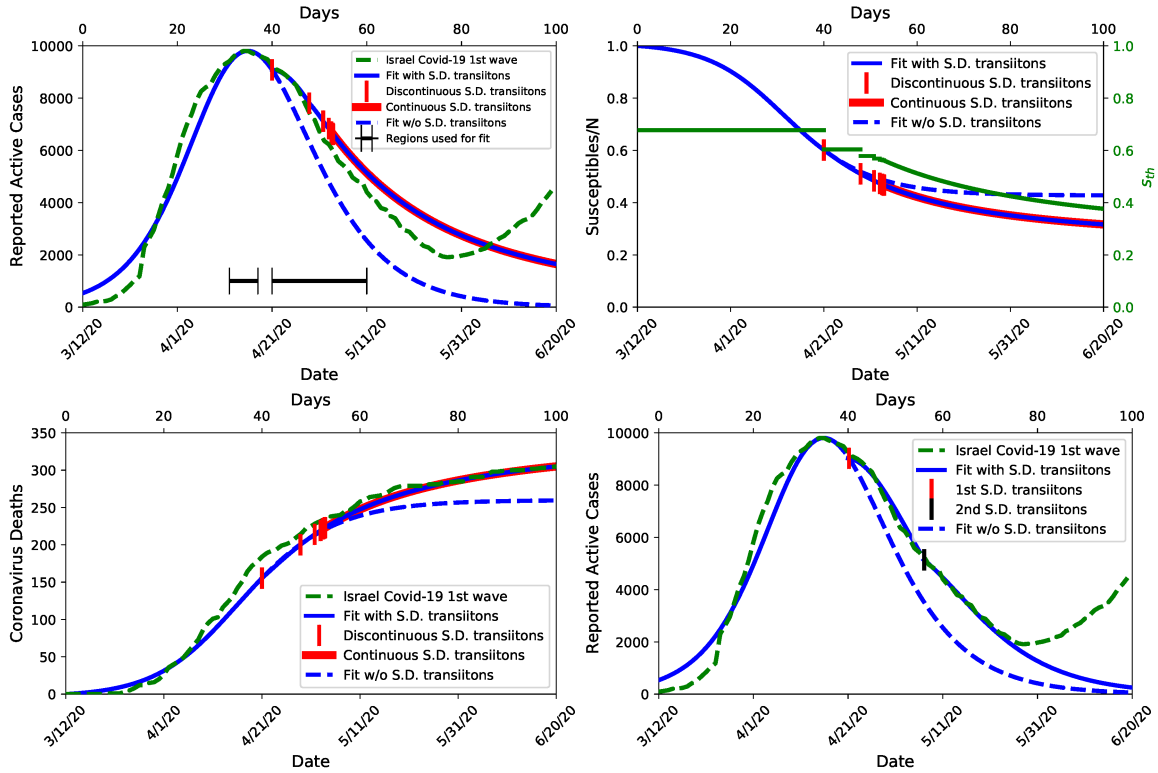


Figure 5. Fit of Israel COVID-19 1st wave. The results are similar to the case of Austria. The fit is valid until the beginning of the 2nd wave about at the 70th day of the first one A) Active cases. A significant deviation exists between reported and calculated active cases even before the start of the second wave. B) Susceptible and s_{th} . The social distancing parameter s_{th} remains a bit higher in Israel rather than in Austria or Germany. C) Coronavirus deaths. The time delay between reported and calculated cases is smaller than in the case of Austria. It can be explained either by late or early reports of coronavirus tests or reported deaths in Israel or Austria. D) Alternative fit with two transitions.

tion from SIR model). Both these scenarios include discontinuous changes in social influence and have the same first transition. All fit attempts of this work need parameters of the SIR model to be constant from pandemic climax (greatest number of infected) till the first transition. Deviations from the fit may reflect a change of regulation and test policies during the first wave.

Analysis of the first wave predicts small, less than 1/10, effective population size in all three tested countries, see Table I. An estimate of effective population size depends on the choice of M - Infected Fatality Rate (IFR). Increase/reduction in M causes proportional reduction/increase in effective population size N and predicted ratio A' between reported and real numbers of infected. These values in Table I correspond to $M = 0.1\%$. The reported value of M for Germany is 0.37%[28]. Thus N and A' maybe about $\times 4$ lower than in Table I. Nevertheless M as low as 0.17% were reported[31]. All other prediction or results of this work, including the graphs, are independent of M . Mortality rate $M > 0.3\%$ causes non-physical $A' < 1$ in case of Israel.

An explanation of low N may be that the ini-

tial lockdown separated the population in disconnected domains[32, 33] and the wave of epidemic occurred in a limited number of domains. The other possible explanation is that a significant part of the population is immune to COVID-19[34]. Finally, SIR approach with quasi-constant parameters may be an oversimplified presentation of reality.

Small effective population size during the first wave may indicate a danger of abrupt transition to a bigger population size when s_{th} reduces below some critical value. It may result in a significant second wave of the epidemic. The critical value of the basic reproduction number was reported for some interaction networks[33, 35], while the majority of the networks lack it[32, 36].

To conclude, this work predicts observable transitions of social distancing and provides tools for quantitative analysis of pandemic waves. Observable phenomena are essential to test the validity of human behavior modeling. The tools, as SIR model itself, contribute to social epidemiology[37] and, to spread of non-contagious but “going-viral” phenomena[38].

Appendix A: Analytic solution of (1)

The first two equations of (1) may be rewritten as:

$$\frac{1}{\beta} \frac{\partial z}{\partial x} z = -\beta A \left(s_{th} + \frac{1}{\beta} z \right) \exp(x), \quad (\text{A1})$$

using transformation $\frac{\partial \log I}{\partial t} = z, \frac{\partial z}{\partial t} = \frac{\partial z}{\partial \log I} \frac{\partial \log I}{\partial t} = \frac{\partial z}{\partial \log I} z, x = \log I$. Integration of (A1) results in:

$$I = I_0 + \frac{1}{A} \left[s_0 - s + s_{th} \log \left[\frac{s}{s_0} \right] \right], \quad (\text{A2})$$

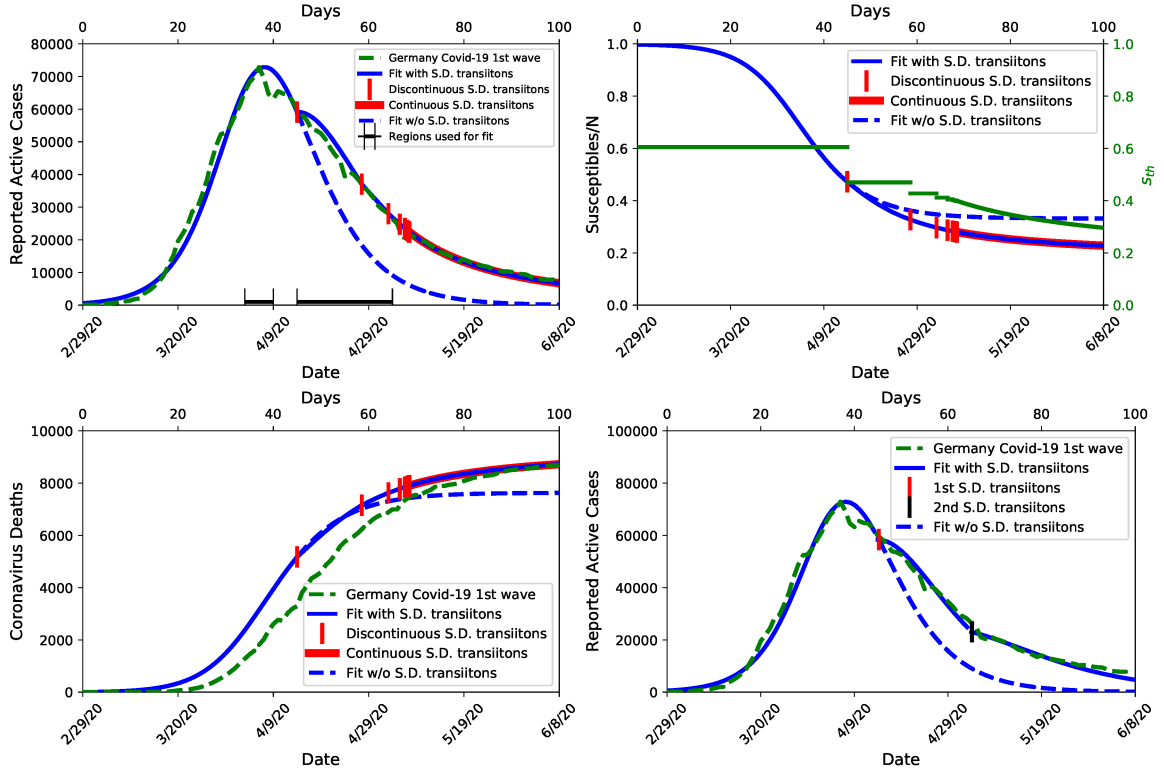


Figure 6. Fit of Germany COVID-19 1st wave. The results are very similar to the case of Austria. A) Active cases B) Susceptible and s_{th} C) Coronavirus deaths. There is a time delay between calculated and reported deaths, like in the case of Austria. D) Alternative fit with two transitions.

	s_0	i_0	γ	s_{th}	β	s_{th}^1	β^1	s_{th}^2	β^2	A	N	A'	M (IFR)	D_1	D_2	A_{open}^1	B_{open}^1
Austria, Fig. 3	0.99	242	0.26	0.56	0.46	0.45	0.46			1.26e-05	8.2e5	10	10^{-3}	32		1.31	5.81
Austria, Fig. 3 A	0.99	242	0.26	0.56	0.46	0.48	0.46			1.26e-05	8.2e5	10	10^{-3}	29		1.84	6.30
Austria, Fig. 3 B	0.99	242	0.26	0.56	0.46	0.48	0.46	0.32	0.46	1.26e-05	8.2e5	10	10^{-3}	29	46	1.84	6.30
Germany, Fig. 6 A,B,C	0.99	578	0.26	0.60	0.43					1.24e-6	1.1e7	14	10^{-3}	45		1.15	5.93
Germany, Fig. 6 D	0.99	578	0.26	0.60	0.43	0.47	0.43	0.33	0.52	1.24e-6	1.1e7	14	10^{-3}	45	65	1.15	5.93
Israel, Fig. 5 A,B,C	1.0	535	0.26	0.68	0.38	0.60	0.38			6.34e-06	4.5e5	3	10^{-3}	40		1.33	4.92
Israel, Fig. 5 D	1.0	535	0.26	0.68	0.38	0.60	0.38	0.50	0.51	6.34e-06	4.5e5	3	10^{-3}	40	56	1.33	4.92

Table I. Parameters of SIRIT model that fit the 1st COVID-19 wave of Austria, Germany and Israel. The parameters may be used to reproduce the figures of the article. For definition of parameters see eq. (1). Besides, D_1 and D_2 are the days of the first and the second (if required) transitions. A_{open}^1, B_{open}^1 are the weights of utility function calibrated for the first transition. An interesting result is really small effective population size N , less than 1/10 of the state population. Greater values of mortality rate M predict even lower values of population size N (increase in M causes proportional reduction in effective population size N and A' ratio between real and reported number of infected). Mortality rate $M > 0.3\%$ causes non-physical $A' < 1$ in case of Israel. The second transition in case of Germany and Israel brings change in β . The results of all three countries are quite similar except A' - ratio between real and reported number of infected.

where (s_0, I_0) are initial values of s and I . To derive (11) for s in the form of Lambert W function (defined as $W(x)$, where $W \exp W = x$) one should rewrite (A2) as:

$$-\frac{s}{s_{th}} \exp \left[-\frac{s}{s_{th}} \right] = -\frac{s_0}{s_{th}} \exp \left[\frac{A(I-I_0)-s_0}{s_{th}} \right]. \quad (\text{A3})$$

The expressions (11) and (A2) provide connection between s and I along population trajectory in (s, I) space that initiates at (s_0, I_0) .

Let us define by (s_t, I_t) values of susceptible ratio s and number of infected I along population trajectory in (s, I) space that initiates at (s_0, I_0) . Then let us calculate the coefficients a, b, c (14) and show that along trajectory (s_t, I_t) they are polynomials of $\log[s_t]$. Derivatives of $\log[s_{min}]$:

$$\log[s_{min}] = \log[s_{th}] + \log[W(f(s_{th}))], \quad (\text{A4})$$

due to s_{th} include derivatives of $\log[s_{th}]$ and derivatives

of $\log [W (f(s_{th}))]$, where:

$$f(s_{th}) = -\frac{s_0}{s_{th}} \exp \left[-\frac{s_0 + AI_0}{s_{th}} \right]. \quad (\text{A5})$$

Let us notice that s_{th} , $f(s_{th})$ and $W (f(s_{th}))$ are constant along trajectory (s_t, I_t) until value of s_{th} changes by a transition. The values $f(s_{th})$ and $W (f(s_{th}))$:

$$f = -\frac{s_0}{s_{th}} \exp \left[-\frac{s_0}{s_{th}} - \frac{AI_0}{s_{th}} \right], \quad (\text{A6})$$

$$W(f) = -\frac{s_{\min}}{s_{th}}, \quad (\text{A7})$$

are constant until a transition takes place, because s_{\min} (A4) is constant along trajectory unless s_{th} changes its value. Besides:

$$-\frac{s_0}{s_{th}} \exp \left[-\frac{AI_0 + s_0}{s_{th}} \right] = \left(-\frac{s_t}{s_{th}} \exp \left[-\frac{s_t}{s_{th}} - \frac{AI_t}{s_{th}} \right] \right) = \text{const.} \quad (\text{A8})$$

because any point (s_t, I_t) can serve as initial value (s_0, I_0) for continuation of the trajectory.

Derivatives of $\log [s_{th}]$ depend only on s_{th} and, so, are constant until s_{th} changes.

Derivatives of $\log [W (f(s_{th}))]$ are:

$$\begin{aligned} \frac{d \log W (f)}{ds_{th}} &= \frac{d \log W (f)}{df} \frac{df}{ds_{th}} \\ \frac{d^2 \log W (f)}{ds_{th}^2} &= \frac{d^2 \log W (f)}{df^2} \left(\frac{df}{ds_{th}} \right)^2 + \frac{d \log W (f)}{df} \frac{d^2 f}{ds_{th}^2} \\ \frac{d^3 \log W (f)}{ds_{th}^3} &= \frac{d^3 \log W (f)}{df^3} \left(\frac{df}{ds_{th}} \right)^3 + \\ & 3 \frac{d^2 \log W (f)}{df^2} \frac{df}{ds_{th}} \frac{d^2 f}{ds_{th}^2} + \frac{d \log W (f)}{df} \frac{d^3 f}{ds_{th}^3} \end{aligned} \quad (\text{A9})$$

Derivatives of $\log W (f)$ due to f are invariant along (s_t, I_t) trajectory, see Appendix B.

Derivatives of f due to s_{th} are polynomials of $\log [s_t]$. Consider the first derivative of (A5) taking into account (A8):

$$\frac{df}{ds_{th}} = gf, \quad (\text{A10})$$

where:

$$g = \left(-\frac{1}{s_{th}} \right) + \left(\frac{s_t + AI_t}{s_{th}^2} \right). \quad (\text{A11})$$

Expression (A2) can be rewritten in the form:

$$AI_t + s_t = AI_0 + s_0 + s_{th} \log \left[\frac{s_t}{s_0} \right] \quad (\text{A12})$$

for trajectory (s_t, I_t) . Plugging (A12) in (A11) results in:

$$g = \left[\left(-\frac{1}{s_{th}} \right) + \left(\frac{AI_0 + s_0 + s_{th} \log \left[\frac{s_t}{s_0} \right]}{s_{th}^2} \right) \right]. \quad (\text{A13})$$

Thus g and its derivatives due to s_{th} are linear function of $\log [s_t]$. The second and the third derivatives then:

$$\frac{d^2 f}{ds_{th}^2} = fg^2 + f \frac{dg}{ds_{th}} \quad (\text{A14})$$

$$\frac{d^3 f}{ds_{th}^3} = fg^3 + 3fg \frac{dg}{ds_{th}} + f \frac{d^2 g}{ds_{th}^2} \quad (\text{A15})$$

are the quadratic and cubic polynomials of $\log [s_t]$.

Appendix B: Derivatives of Lambert W function

All derivatives of W due to f are constant along any trajectory in (s, i) space:

$$W \exp [W] = f, \quad (\text{B1})$$

$$\frac{d \log W}{df} = \frac{1}{f(1+W)}, \quad (\text{B2})$$

$$\frac{d^2 \log W}{df^2} = -\frac{1}{f} \frac{d \log W}{df} - fW \left[\frac{d \log W}{df} \right]^3, \quad (\text{B3})$$

$$\begin{aligned} \frac{d^3 \log W}{df^3} &= \frac{1}{f^2} \frac{d \log W}{df} - \frac{1}{f} \frac{d^2 \log W}{df^2} - W \left[\frac{d \log W}{df} \right]^3 - \\ & fW \left[\frac{d \log W}{df} \right]^4 - 3fW \left[\frac{d \log W}{df} \right]^2 \frac{d^2 \log W}{df^2}. \end{aligned} \quad (\text{B4})$$

The final expressions are invariant until s_{th} changes because they depend on f and W only, see (A7).

Appendix C: Final expressions for a,b,c

The first:

$$a = -\frac{AI_0 - s_{\min} + s_{th} \log \left(\frac{s}{s_0} \right) + s_0}{s_{th} (s_{th} - s_{\min})} \quad (\text{C1})$$

The second:

$$b = -\frac{1}{2s_{th}^2 (s_{th} - s_{\min})^3} \times \quad (\text{C2})$$

$$\left(AI_0 - s_{\min} + s_{th} \log \left(\frac{s}{s_0} \right) + s_0 \right) \times$$

$$\left(s_{\min} (AI_0 - s_{\min} + s_0) + 2s_{\min} s_{th} + s_{\min} s_{th} \log \left(\frac{s}{s_0} \right) - 2s_{th}^2 \right)$$

and

$$\begin{aligned}
c = & -\frac{1}{6s_{\text{th}}^3(s_{\text{th}} - s_{\text{min}})^5} \left[\left(AI_0 - s_{\text{min}} + s_{\text{th}} \log\left(\frac{s}{s_0}\right) + s_0 \right) (-3s_{\text{min}}s_{\text{th}}^2(3AI_0 - 5s_{\text{min}} + 3s_0)) + \right. \\
& s_{\text{min}}s_{\text{th}}(AI_0 - s_{\text{min}} + s_0)(AI_0 + 8s_{\text{min}} + s_0) + s_{\text{min}}s_{\text{th}} \log\left(\frac{s}{s_0}\right) \times \\
& \left(s_{\text{th}}(2AI_0 + 7s_{\text{min}} + 2s_0) + 4s_{\text{min}}(AI_0 - s_{\text{min}} + s_0) + s_{\text{th}} \log\left(\frac{s}{s_0}\right)(2s_{\text{min}} + s_{\text{th}}) - 9s_{\text{th}}^2 \right) + \\
& \left. 2s_{\text{min}}^2(AI_0 - s_{\text{min}} + s_0)^2 - 12s_{\text{min}}s_{\text{th}}^3 + 6s_{\text{th}}^4 \right]
\end{aligned} \tag{C3}$$

-
- [1] R. M. May and R. M. Anderson, *Phil. Tran. R. Soc. Lon. B* **321**, 565 (1988).
- [2] C. Bauch, A. d’Onofrio, and P. Manfredi, in *Modeling the Interplay Between Human Behavior and the Spread of Infectious Diseases*, edited by P. Manfredi and A. D’Onofrio (Springer, 2013), pp. 1–19.
- [3] R. M. Anderson, H. Heesterbeek, D. Klinkenberg, and T. D. Hollingsworth, *The Lancet* **395**, 931 (2020-03).
- [4] A. Atkeson (2020-03), URL <http://www.nber.org/papers/w26867.pdf>.
- [5] P. Poletti, B. Caprile, M. Ajelli, A. Pugliese, and S. Merler, *J. Theor. Biol.* **260**, 31 (2009).
- [6] T. C. Reluga, *PLoS Comp. Biol.* **6**, e1000793 (2010).
- [7] E. P. Fenichel, C. Castillo-Chavez, M. G. Ccedia, G. Chowell, P. A. G. Parra, G. J. Hickling, G. Holloway, R. Horan, B. Morin, C. Perrings, et al., *Proc. Nat. Acad. Sci.* **108**, 6306 (2011).
- [8] L. Lopez and X. Rodo, *Nature Human Behaviour* **4**, 746 (2020-07).
- [9] M. Farboodi, G. Jarosch, and R. Shimer (2020), URL <https://www.nber.org/papers/w27059.pdf>.
- [10] F. Alvarez (2020), URL <https://www.nber.org/papers/w26981.pdf>.
- [11] Z. Wang, M. A. Andrews, Z.-X. Wu, L. Wang, and C. T. Bauch, *Phys. Life Rev.* **15**, 1 (2015).
- [12] P. C. Ventura da Silva, F. Velasquez-Rojas, C. Connaughton, F. Vazquez, Y. Moreno, and F. A. Rodrigues, *Phys. Rev. E* **100** (2019).
- [13] W. O. Kermack and A. G. McKendrick, *Proc. R. Soc. Lon. A* **115**, 700 (1927).
- [14] M. E. J. Newman, *Phys. Rev. E* **66** (2002).
- [15] J. Tanimoto, *Evol. Games with Sociophysics* **17**, 155 (2018).
- [16] D. McAdams, arXiv:2006.10109 [econ] (2020), 2006.10109.
- [17] M. Eichenbaum, S. Rebelo, and M. Trabandt (2020), URL <http://www.nber.org/papers/w26882.pdf>.
- [18] F. Toxvaerd (2020), URL <http://www.econ.cam.ac.uk/.../cwpe2021.pdf>.
- [19] L. D. Landau and E. M. Lifshitz, *Statistical Physics: Volume 5*, vol. 5 (Elsevier, 2013).
- [20] M. Perc, **380**, 2803 (2016).
- [21] M. Levy, **57**, 71 (2005).
- [22] J. A. Kelso, **246**, R1000 (1984).
- [23] P. A. Diamond and E. Maskin, *Bell J. Econ.* **10**, 282 (1979).
- [24] F. Wang, *Col. Math. J.* **41**, 156 (2010).
- [25] T. Reluga, *J. Theor. Biol.* **229**, 249 (2004).
- [26] J. Lehtonen, *Methods in Ecology and Evolution* **7**, 1110 (2016).
- [27] E. Dong, H. Du, and L. Gardner, *The Lancet infectious diseases* **20**, 533 (2020).
- [28] H. Streeck, B. Schulte, B. Kueimmerer, E. Richter, T. Hoeller, C. Fuhrmann, E. Bartok, R. Dolscheid, M. Berger, L. Wessendorf, et al. (2020), URL <http://medrxiv.org/lookup/doi/10.1101/2020.05.04.20090076>.
- [29] K. Kuga, J. Tanimoto, and M. Jusup, *J. Theor. Biol.* **469**, 107 (2019).
- [30] M. M. Bohmer, U. Buchholz, V. M. Corman, M. Hoch, K. Katz, D. V. Marosevic, S. Bohm, T. Woudenberg, N. Ackermann, R. Konrad, et al., *The Lancet Infectious Diseases* **20**, 920 (2020).
- [31] E. Bendavid, B. Mulaney, N. Sood, S. Shah, E. Ling, R. Bromley-Dulfano, C. Lai, Z. Weissberg, R. Saavedra-Walker, J. Tedrow, et al. (2020), URL <http://medrxiv.org/lookup/doi/10.1101/2020.04.14.20062463>.
- [32] D. S. Callaway, M. E. J. Newman, S. H. Strogatz, and D. J. Watts, *Phys. Rev. Lett.* **85**, 4 (2000).
- [33] C. Warren, L. Sander, and I. Sokolov, *Phys. Rev. E* **66** (2002).
- [34] J. Mateus, A. Grifoni, A. Tarke, J. Sidney, S. I. Ramirez, J. M. Dan, Z. C. Burger, S. A. Rawlings, D. M. Smith, E. Phillips, et al., *Science* p. eabd3871 (2020).
- [35] L. Sander, C. Warren, I. Sokolov, C. Simon, and J. Koopman, *Math. Biosci.* **180**, 293 (2002).
- [36] M. Newman, *SIAM Rev.* **45**, 167 (2003).
- [37] C. T. Bauch and A. P. Galvani, *Science* **342**, 47 (2013).
- [38] R. J. Shiller, *Am. Econ. Rev.* **107**, 967 (2017).